

# Nafion<sup>®</sup> 117 modified by low dose EB irradiation: surface structure and physical properties

Lois J. Hobson,<sup>a</sup> Hideyuki Ozu,<sup>a</sup> Masanori Yamaguchi,<sup>b</sup> Miho Muramatsu<sup>a</sup> and Shuji Hayase<sup>\*c</sup>

<sup>a</sup>Corporate Research and Development Centre, Toshiba Corporation, 1 Komukai, Toshiba-cho, Saiwai-ku, Kawasaki 212-8582, Japan

<sup>b</sup>Ushio Inc., 1194, Sazuchi, Bessho-cho, Himeji, Hyogo 671-0224, Japan

<sup>c</sup>Kyushu Institute of Technology, Graduate School of Engineering and Systems Engineering, 1-1 Hibikino, Wakamatsu-ku, Kitakyushu 808-0196, Japan.  
E-mail: hayase@life.kyutech.ac.jp

Received 1st October 2001, Accepted 11th March 2002

First published as an Advance Article on the web 17th April 2002

Recent progress in the treatment of Nafion<sup>®</sup> 117 film by low dose electron beam (EB) exposure is described. The effect of EB exposure between 0 and 400  $\mu\text{C cm}^{-2}$  doses is discussed on a structural level and a dual reaction mechanism, involving cleavage of the hydrophilic side chain and subsequent formation of  $-\text{CO}_2\text{H}$  units at the site of the polymer backbone, proposed for this system. This work was extended by consideration of the effects of EB irradiation in the presence of different oxygen concentrations, 50 ppm, 550 ppm and 2000 ppm. From these studies we conclude that low dose EB exposure facilitates replacement of the sulfuric acid moieties, located at the terminus of the Nafion<sup>®</sup> side chain, with carboxylic acid units as the dominant hydrophilic group found in the pores of the ion channels at the Nafion<sup>®</sup> surface. It has been demonstrated that by increasing the degree of carboxylic acid formation at the site of the polymer backbone the conductivity of the resultant material can be buffered sufficiently so as to compensate for the effect of the subsequent cleavage of the hydrophilic side chains. This result not only confirms the irradiation mechanism postulated but allows significant advantages in the development of membranes with properties optimised for DMFC performance.

## 1. Introduction

The field of fuel cell technology covers a wide range of systems, applications and performance specifications but despite this diversity, the basic concepts remain common. As such, key developments in fundamental technology, whether in terms of components, device fabrication or design, can have a significant impact industry wide. As fuel cells move swiftly into the commercial domain, with applications ranging from transportation<sup>1,2</sup> and stationary power supply<sup>3</sup> to small portable electronic devices,<sup>4,5</sup> the polymer electrolyte membrane is highlighted as the current limiting factor regarding exploitation of this technology. With specific reference to the direct methanol fuel cell (DMFC), performance is largely dependent on the selective permeability characteristics of the membrane,<sup>6,7</sup> two electrodes separated by a polymer electrolyte membrane forming the core components of the DMFC. Considering the mode of DMFC operation, methanol enters the system at the anode, where it is oxidised generating carbon dioxide [ $\text{CH}_3\text{OH} + \text{H}_2\text{O} \rightarrow \text{CO}_2 + 6\text{H}^+ + 6\text{e}^-$ ], while the corresponding reduction process takes place at the cathode, [ $4\text{H}^+ + \text{O}_2 + 4\text{e}^- \rightarrow 2\text{H}_2\text{O}$ ]. However, due to the similar composition of the two electrodes, if methanol crossover through the polymer electrolyte membrane is experienced then methanol oxidation can also occur at the cathode, dramatically reducing overall performance. Although a number of factors can influence DMFC performance, methanol crossover actively decreases the open current voltage (OCV) of the cell. Hence improvements in the selective permeability characteristic of the membrane, facilitating the passage of water but restricting methanol, can produce significant gain in terms of device performance.

Nafion<sup>®</sup> to date remains the most widely used commercial membrane for DMFC applications. Its unique structure

provides inherent high conductivity and good mechanical properties which are as yet hard to replicate in a material more suited to fuel cell applications. The high extent of methanol permeability reported for Nafion<sup>®</sup> based DMFC systems remains problematic. Developed by Du Pont<sup>®</sup> in 1962, Nafion<sup>®</sup> is best characterised as a copolymer of tetrafluoroethylene and an ethenesulfonic acid. The resultant structure can be considered as having two distinct regions, the hydrophobic PTFE backbone and the hydrophilic, sulfonic acid terminated, perfluorinated side chains. Due to its high cation selectivity and excellent chemical and thermal stability, Nafion<sup>®</sup> film has found a wide range of industrial applications. As a direct consequence, its physical properties, particularly morphology, have been the subject of numerous publications. Using techniques ranging from IR,<sup>8-10</sup> NMR and positron annihilation spectroscopy<sup>11</sup> to atomic force microscopy (AFM),<sup>12</sup> neutron and X-ray scattering<sup>13,14</sup> and molecular modelling,<sup>15</sup> Nafion<sup>®</sup> film has been shown to adopt a phase segregated structure, with a series of internal ion channels, accounting for its high conductivity.

We have previously proposed the use of low dose EB irradiation to establish a thin methanol impermeable barrier layer at the Nafion<sup>®</sup> surface.<sup>16-18</sup> This approach relies on the ability of EB exposure to reduce the size of the surface pores of the ion channel, thus selectively restricting the passage of methanol through the film whilst allowing water to move freely. The EB system used (MIN-EB-Lab, Ushio Inc., Japan) allows the films to be irradiated at significantly lower acceleration voltages than used by conventional apparatus. Working at an accelerating voltage of 40 kV we calculate an EB penetration depth of  $< 5 \mu\text{m}$ ; in marked contrast with conventional systems where 100 kV produces a penetration depth in excess of  $100 \mu\text{m}$ . Preliminary experimental results showed that exposure to low dose irradiation is able to significantly reduce the methanol

permeability of Nafion<sup>®</sup>117, *i.e.* 600  $\mu\text{C cm}^{-2}$  dose reducing methanol crossover in the cell to 7% of that of the untreated film. Subsequent experiments have produced materials in which a reduction in methanol permeability is combined with high conductivity. Simple device trials, based on these materials, have also established the viability of EB treated Nafion<sup>®</sup>117 film as a core fuel cell component,<sup>16</sup> improvements, in terms of both increased power output and current density range, over that of the parent film having been observed.<sup>17</sup>

Use of such a barrier type strategy provides the best chance of maintaining the inherent conductivity of the parent material and has previously been adopted, by us and others, in applications to fuel cell technology. For example, the introduction of a thin layer of polybenzimidazole (PBI) at the Nafion<sup>®</sup> surface was shown to reduce methanol permeability whilst maintaining proton conductivity at a level comparable to the parent material.<sup>19</sup> Other recent publications describing a similar approach include plasma polymerisation,<sup>20</sup> or the application of a PBI layer by spray coating or the layering of solution cast films.<sup>21</sup>

Here we discuss the effects of low dose EB exposure on Nafion<sup>®</sup>117 film at a molecular level, attempting to relate the mechanism of irradiation to the physical properties observed. We draw on experimental data taken over a range of sample and irradiation conditions, aiming at a comprehensive understanding of the structure–property correlation for this material. Regarding the likely mechanism of irradiation, parallels are drawn between the exposure of Nafion<sup>®</sup> to low dose EB irradiation and the traditional EB treatment of bulk polymers with structural similarities. Herein we report the findings of a series of new irradiation experiments, designed to lend further support to our mechanistic evaluation, and in combination with previous data we aim to present an overall picture of the effects of low dose EB irradiation, highlighting features most applicable to fuel cell technology.

## 2. Experimental

### 2.1 Nafion<sup>®</sup> film

All experiments were carried out using Nafion<sup>®</sup>117 film (0.2 mm).

### 2.2 EB exposure apparatus

**2.2.1 Standard exposure at <200 ppm oxygen.** Nafion<sup>®</sup>117 films were exposed to low dose electron beam irradiation (Min-EB-Lab, Ushio Inc., Japan), at room temperature, working at an accelerating voltage of 35 kV, unless otherwise stated. The Min-EB-Lab is fitted with an electron beam tube of dimensions 45 × 144 mm, has a silicon electron window (3  $\mu\text{m}$ ) and a voltage range of 35 to 75 kV. The instrument uses a multi-tube module system, where 7 tubes give an effective irradiation width of 125 mm with a uniformity of  $\pm 15\%$ . Exposure was carried out at an accelerating voltage of 35 kV, with a tube current of 300  $\mu\text{A}$  per tube and scan speed of 3  $\text{m min}^{-1}$ ; resulting in a dose per scan rate of 2.5  $\mu\text{C cm}^{-2}$ . Irradiation was carried out in an atmosphere containing less than 200 ppm oxygen. The gap between the sample plate and the electron window was set at 12 mm. Films were fixed on to the sample plate using adhesive tape to secure all four edges. This masked region was not exposed and was removed prior to analysis of the film. Under these experimental conditions, for Nafion<sup>®</sup> film (density = 2, stoichiometry =  $\text{C}_{19}\text{F}_{38}\text{O}_5\text{SH}$ ) the penetration depth of the irradiation was calculated to be 1.5  $\mu\text{m}$ .

**2.2.2 Exposure at known oxygen concentrations.** An oxygen meter was added to the experimental arrangement, situated

close the EB source. As shown in Fig. 9, the EB-MIN-Lab has two air inlet ports located at the rear of the machine, which feed into two load lock chambers. A nitrogen gas flow is maintained at the EB source to cool the electron window.

To increase the oxygen content within the irradiation chamber, airflow to the inlet ports was increased using an external airflow pump. During irradiation the two gates dividing the EB chamber and loadlock chambers are open allowing mixing of the gases. These mixed gases are removed from the box *via* a vented outlet port to the rear of the irradiation chamber.

### 2.3 Film analysis

The exposed films were analysed by IR reflectance (ATR) spectroscopy at three stages in the experiment, (i) directly after EB exposure, (ii) after subsequent hydration in distilled water at room temperature for 48 hours and (iii) after subsequent dehydration at 100 °C for 16 hours, using a Bio-Rad FTS 6000 Stingray instrument. Data were taken between 700 and 4000  $\text{cm}^{-1}$  over 250 scans and compared with the parent material.

Subsequently the properties of the film itself, in terms of conductivity, methanol permeability, percentage water uptake and shrinkage were analysed and contrasted with the untreated material. Methanol crossover within the film was measured by gas chromatography. 5  $\mu\text{L}$  portions were extracted from the cathode reservoir of a simplified DMFC and analysed for their percentage methanol content. Conductance of the film samples was determined from impedance data taken after an appropriate equilibrium period, at a frequency of 1 kHz using a Hewlett Packard 4192A-LF impedance analyser.

### 2.4 Film preparation

The films irradiated were pre-treated in various ways. Hydrated films (HT) were prepared by boiling in distilled water between 95–100 °C for one hour. Other samples were pre-cleaned using an acid treatment<sup>22</sup> (PT) and a proportion of these subsequently pressed at 125 °C to alter the hydration state of the film (PT/P). Such samples were used to demonstrate that the hydration state of the film during exposure has a major influence on the properties of the subsequent material.

## 3 Results and discussion

### 3.1 Nafion<sup>®</sup> film

In this paper our interest lies in the properties of the commercial polymer membrane Nafion<sup>®</sup>117 (0.2 mm), rather than those of the Nafion<sup>®</sup> resin. Current polymer processing of this material results in a certain degree of orientation within the membrane. Considering the film in two dimensions, this is exemplified by the difference in swelling upon hydration along the *x*- and *y*-axis. Experimentally we observe a difference in expansion; 11% to 16% along the *x*- and *y*-axis after aqueous treatment (1 h/100 °C), increasing to 13% and 22% upon acid pre-cleaning.<sup>22</sup> It is worthy of note that these values were reproducible between different film batches within  $\pm 0.5\%$ . In order to reduce any consequential effects regarding reproducibility of conductance measurements, in all cases the electrodes were placed parallel with the direction of maximum film expansion, easily observed in the hydrated material.

### 3.2 Effects of EB irradiation

From a combination of several series of experimental data, taken at 0–600  $\mu\text{C cm}^{-2}$  (dehydrated film),<sup>17</sup> 0–100  $\mu\text{C cm}^{-2}$  (hydrated film)<sup>16</sup> and 0–400  $\mu\text{C cm}^{-2}$  (hydrated film, presented here), we conclude that for low dose EB irradiation, operating at an accelerating voltage of 35 kV, both hydrophilic and

hydrophobic regions of the polymer undergo modification. IR reflectance (ATR) spectroscopy has been established as a valuable technique for surface analysis of Nafion<sup>®</sup> films. We have previously reported<sup>16</sup> that for Nafion<sup>®</sup> film exposed to EB irradiation we detect signals in the IR spectra corresponding to the literature values denoted for the parent material.<sup>8,9</sup>

Considering the above data series, in all cases a reduction in signal intensity with progressive EB exposure (in the range 0–300  $\mu\text{C cm}^{-2}$ ) can be observed for peaks centred at 1060  $\text{cm}^{-1}$ , assigned to the  $\text{SO}_3^-$  unit, and at 980  $\text{cm}^{-1}$  and 968  $\text{cm}^{-1}$ , assigned to the C–O–C stretching mode. In contrast the intensity of the C–F stretching band, which dominates the region 1100–1300  $\text{cm}^{-1}$ , remains largely unaffected. The C–O–C stretching modes at 980 and 968  $\text{cm}^{-1}$  correspond to units in the hydrophilic side chain; likewise the  $\text{SO}_3^-$  symmetrical stretching vibrations, observed as a strong band at 1060  $\text{cm}^{-1}$ , and associated stretching modes at 1320 and 1210  $\text{cm}^{-1}$ , assigned to the terminal pendant  $\text{SO}_3\text{H}$  group. From these data we conclude that the hydrophilic  $(-\text{OCF}_2-\text{C}(\text{CF}_3)-\text{F})_n-\text{OCF}_2\text{CF}_2-\text{SO}_3\text{H}$  side chains of the polymer are lost as a function of EB exposure dose. The intensities of the two signals at 980  $\text{cm}^{-1}$  and 968  $\text{cm}^{-1}$ , assigned to the stretching vibrations of the C–O–C units of the side chain, are shown to decrease at the same rate as a function of EB dose. The peak at 1060  $\text{cm}^{-1}$ , assigned to the terminal  $\text{SO}_3^-$  end group, also displays a similar reduction in signal intensity, Fig. 1.

From these observations we can conclude that the entire side chain is lost as a function of EB exposure dose (a), rather than partial fragmentation at either (b) or (c) sites, as shown in Fig. 2.

This is an important observation as it allows us to assume that we are approaching complete side chain removal when we start to observe a plateau in the intensity of these signals above 300  $\mu\text{C cm}^{-2}$ . Additionally the new experimental data reported here, the irradiation of hydrated films (pre-treated with acid<sup>22</sup>) at 0–400  $\mu\text{C cm}^{-2}$  doses and 35 kV, show that these signals are unaffected by post irradiation treatment. Indeed for these signals shown in Fig. 1, after dehydration of the

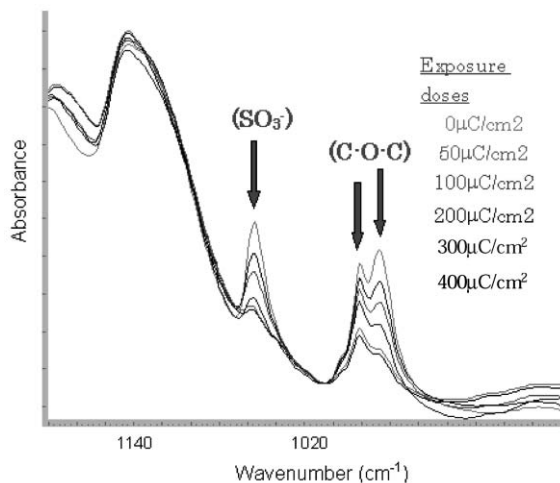


Fig. 1 IR spectra (870–1100  $\text{cm}^{-1}$ ) for samples irradiated at 0–400  $\text{mC cm}^{-2}$ . The order of the lines at the arrows corresponds to that of the exposure doses.

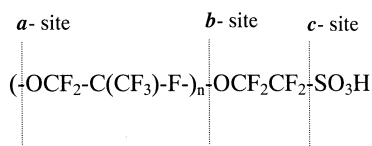


Fig. 2 Possible sites of partial fragmentation resulting from EB exposure.

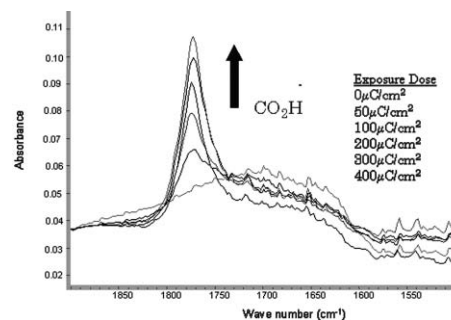


Fig. 3 IR spectra for dehydrated samples (1500–1900  $\text{cm}^{-1}$ ). The order of the lines at the arrow corresponds to that of the exposure doses.

irradiated films at 100 °C for 16 h, the IR spectra are identical to those recorded (i) directly after EB exposure and (ii) after hydration (at room temperature with distilled water for 48 h) but prior to dehydration.

In contrast, for treatment of Nafion<sup>®</sup> 115 film by conventional EB techniques,<sup>23</sup> where higher accelerating voltages result in significantly greater penetration depths, no loss of the side chain was reported for exposure doses in the 0–20 mRad range, corresponding to 0–40  $\mu\text{C cm}^{-2}$ . Nafion 115 and 117 have the same basic structure but differ in terms of film thickness, 150  $\mu\text{m}$  and 200  $\mu\text{m}$ , respectively. However other aspects of our data (working in at a comparable dose), regarding irradiation effect on the polymer backbone, are in complete agreement with literature data reported using conventional instrumentation. For instance, observation of the formation of carboxylic acid groups at the site of the polymer backbone in the hydrated films at doses above 20  $\mu\text{C cm}^{-2}$ .<sup>18</sup> Turning to consider this region of the spectrum, 1500–1900  $\text{cm}^{-1}$  (Fig. 3), for materials irradiated in the hydrated state at 0–400  $\mu\text{C cm}^{-2}$  similar conclusions can be drawn. The peak centred at 1770  $\text{cm}^{-1}$ , located in the region where stretching vibrations of the C=O (acid) and  $\text{CF}_2-\text{CF}_2$  groups overlap, is conclusively assigned to the C=O (acid) stretching mode. This was proven to be so by treatment of the film with 1 M sodium hydroxide solution. Re-analysis after subsequent dehydration indicated the expected shift from the acid C=O stretch (1770  $\text{cm}^{-1}$ ) by almost 100  $\text{cm}^{-1}$  to 1680  $\text{cm}^{-1}$ , the position of the C=O stretch for  $-\text{COONa}$ .

Fig. 3 shows that the intensity of the signal centred at 1770  $\text{cm}^{-1}$ , assigned to the formation of carboxylic acid groups at the site of side chain scission on the polymer backbone, increases with increasing irradiation dose, up to 300  $\mu\text{C cm}^{-2}$ . As an increase in the  $-\text{CO}_2\text{H}$  content of the polymer should improve conductivity of the material, we attempted to identify the limiting factors for this mechanism, discussed later.

From analysis of the IR data presented we can conclude that over this exposure range there are two competing processes associated with EB exposure:  $\text{CO}_2\text{H}$  groups are generated within the polymer structure and the hydrophilic  $(-\text{OCF}_2-\text{C}(\text{CF}_3)-\text{F})_n-\text{OCF}_2\text{CF}_2-\text{SO}_3\text{H}$  side chains are lost. Therefore we propose a final structure of the irradiated Nafion<sup>®</sup> film with a proportion, dependent upon irradiation conditions, of the  $-\text{SO}_3^-$  units at the surface replaced by  $-\text{CO}_2\text{H}$  groups. Hence we can consider the ion channels of the polymer as shown schematically in Fig. 4.

### 3.3 Physical properties resulting from irradiation

The opposing effects of these mechanisms on the physical properties focused on in this application, namely conductivity, methanol crossover and water content, means that we expect to observe a complex relationship with respect to irradiation dose, Fig. 5.

EB dose–conductance profiles (conductance recorded across the film surface) provide further evidence to substantiate the

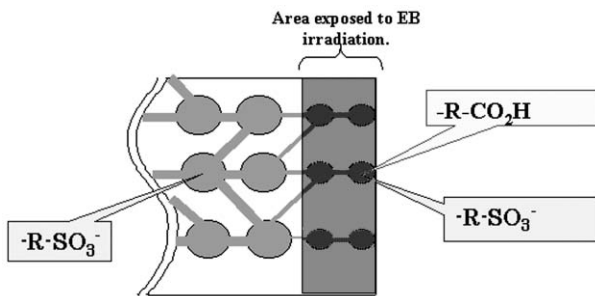


Fig. 4 Composition of ion channels of Nafion® film after EB irradiation.

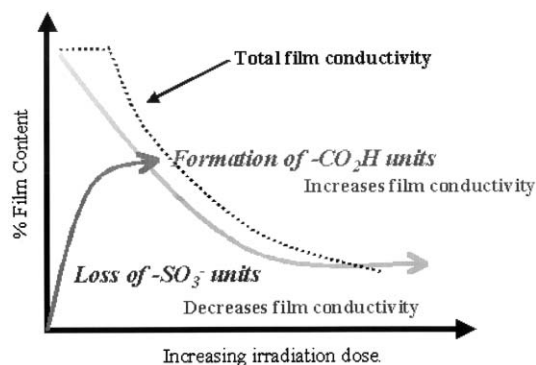


Fig. 5 Schematic diagram to illustrate the balance of conductivity.

conclusions drawn from IR analysis. Fig. 6 shows the relationship between irradiation dose and conductance (relative to hydrated Nafion® 117) calculated from impedance measurements taken both (a) across the film surface and (b) through the film cross section. The two profiles displayed are dramatically different and previous studies have shown that only measurements taken through the film cross section (b) provide an accurate interpretation of the role of the membrane within the DMFC.

A gradual decrease in conductivity is shown for progressive side chain loss in Fig. 6(a) while in contrast Fig. (b) depicts a dramatic drop in conductance corresponding to an irradiation dose of 150–200  $\mu\text{C cm}^{-2}$ . In both cases the difference in conductance between one side (A) and two side (AB) exposure is not as great as initially expected. Referring to Fig. 6(b), significantly we note that the effect of 100  $\mu\text{C cm}^{-2}$  irradiation on each side (AB) is by no means equivalent to 200  $\mu\text{C cm}^{-2}$  irradiation on one side (A). In terms of conductivity, from this series of films A = 150  $\mu\text{C cm}^{-2}$  is identified as being of potential interest with respect to DMFC application. We also highlight the exposure ranges of A = 150–200  $\mu\text{C cm}^{-2}$  and AB = 100–200  $\mu\text{C cm}^{-2}$  as of interest in terms of future EB irradiation experiments using these conditions.

Having shown that we have films of potential interest for fuel cell applications we progressed to investigate the permeability of these materials towards methanol. The plots of conductance versus methanol crossover are shown in Fig. 7 for the samples of prime interest. The sample A = 150  $\mu\text{C cm}^{-2}$  effectively reduces methanol cross-over in the order of 50% when compared with data recorded for hydrated Nafion® 117, while maintaining conductance at a similar level.

Analysis of IR spectra obtained in the three possible states, directly after irradiation, hydrated and dehydrated also allows us to look at the effect of EB dose on the water content and uptake capabilities of the film.

### 3.4 Proposed mechanism of irradiation

In considering the likely mechanism of EB exposure for this system we look to the literature describing the conventional exposure of polytetrafluoroethylene (PTFE) by EB

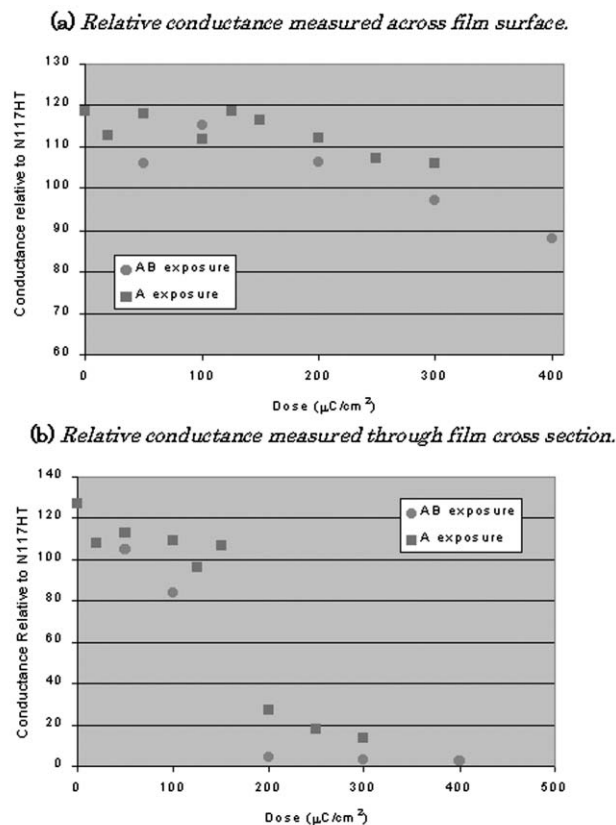


Fig. 6 Conductance–EB dose profiles. Measurements taken (a) across film surface, (b) through film cross-section.

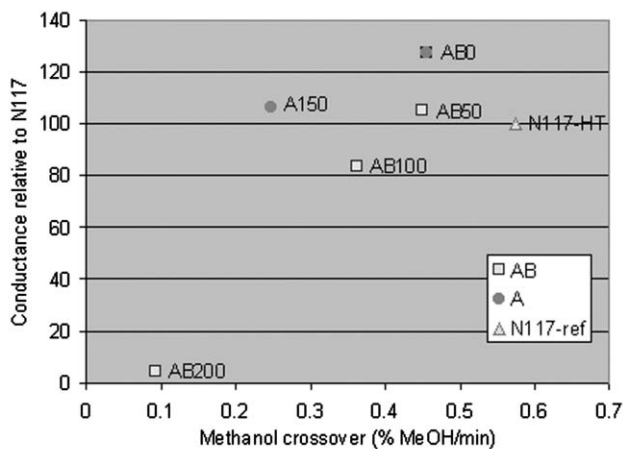


Fig. 7 Conductance versus methanol crossover.

irradiation.<sup>24</sup> In our experiments, from the available IR (ATR) data we conclude that the Nafion® side chain is removed as a result of EB exposure, leaving the backbone of the polymer. Hence this corresponds to the first stage of the classic irradiation of PTFE, where chain scission leads to an initial radical structure.<sup>25</sup> For PTFE it is accepted that in the presence of air, subsequently radiation induced radicals react with oxygen to form acid fluoride groups (-COF). The -COF groups are then hydrolysed to -COOH units in the presence of water, resulting in the formation of carboxylic acid groups in the polymer.<sup>26</sup> This seems a reasonable for the EB irradiation of Nafion®, providing adequate explanation for the phenomena observed, Fig. 8.

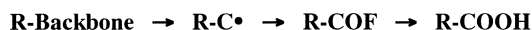


Fig. 8 Summary of proposed mechanism of irradiation.

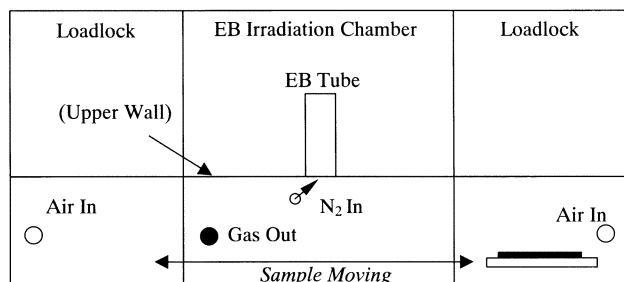


Fig. 9 Front View of Min-EB-Lab

If this is the case then, as the films are irradiated in the hydrated state, facilitating the final hydration step, the limiting factor for the generation of -COOH units is likely to be the availability of oxygen. Therefore a series of experiments were designed to investigate the effect of oxygen concentration during EB exposure.

### 3.5 Effect of oxygen concentration during exposure

Using the basic PTFE system and traditional irradiation techniques it has been established that the atmospheric conditions under which irradiation takes place are crucial in terms of the products formed. Lappan *et al.* demonstrated the effects of both the presence of ammonia gas<sup>26</sup> and working under vacuum<sup>27</sup> on the resultant products of EB exposure. In our experiments, up until now all materials were irradiated under atmospheric conditions with oxygen levels less than 200 ppm. Oxygen levels were not recorded more precisely which, in view of the proposed mechanism of irradiation, we now suspect accounts for the slight differences observed between samples prepared under seemingly identical conditions on different days.

The configuration of the MIN-EB-Lab is shown in Fig. 9; for these experiments an oxygen meter is added close to the irradiation source and air is pumped through the system using the inlet and outlet ports indicated.

From the data presented in section 2.3 we determined that for our standard irradiation conditions the range of exposure dose of interest lies between 100 and 200  $\mu\text{C cm}^{-2}$ . This range includes the dramatic drop in conductivity, attributed to loss of the majority of the Nafion<sup>®</sup> side chains. As previously our only criterion concerning oxygen concentration was a ceiling of 200 ppm we selected three oxygen levels, (50 ppm, 550 ppm and 2000 ppm) under which experimental trials at 0, 50, 100, 150 and 200  $\mu\text{C cm}^{-2}$  EB doses would be carried out. All films were exposed on one side, in the hydrated state after acid cleaning.<sup>22</sup> IR reflectance (ATR) spectroscopy measurements

**Table 1** Effect of exposure dose<sup>a</sup> and oxygen concentration on conductivity

Samples	Oxygen (ppm)	Dose/ $\mu\text{C cm}^{-2}$	Conductance relative to N117HT (%)
June			
2001-EB			
OC-AO	Reference film (N117PT)	0	88
OC-A1	~50	50	101
OC-A2	~50	100	98
OC-A3	~50	150	33
OC-A4	~50	200	14
OC-A5	~550	50	116
OC-A6	~550	100	93
OC-A7	~550	150	99
OC-A8	~550	200	65
OC-A9	~2000	50	107
OC-A10	~2000	100	116
OC-A11	~2000	150	89
OC-A12	~2000	200	103

<sup>a</sup>All samples exposed on one side only (A).

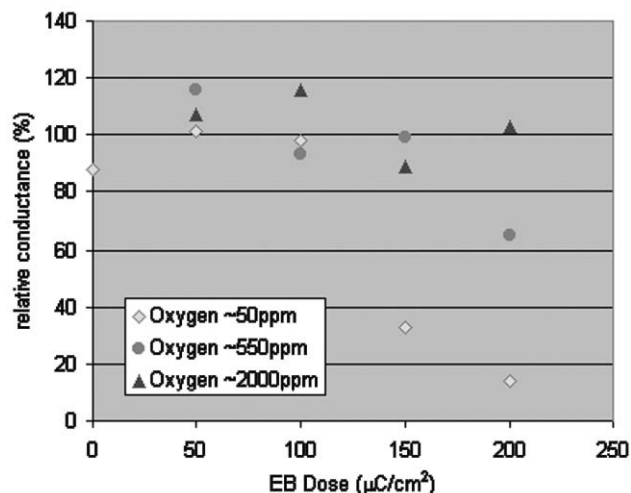


Fig. 10 Conductance against exposure dose as a function of oxygen content.

were taken at the same three stages described in section 2.2. The films were also analysed to determine their conductance relative to that of Nafion<sup>®</sup>117, using a previously established protocol.<sup>17</sup> These results, quoted in Table 1, show that the properties of the irradiated materials are heavily dependent on the atmospheric conditions during irradiation.

Viewing the data shown in Table 1 in terms of three exposure series (0–200  $\mu\text{C cm}^{-2}$ ) taken in the presence of 50 ppm, 550 ppm and 2000 ppm of oxygen, the elimination of the dramatic conductance drop between 100 and 150  $\mu\text{C cm}^{-2}$  shown for 50 ppm oxygen is clearly shown, Fig. 10. Even at 550 ppm oxygen the decrease shown, in the range of from 100 to 60%, is moved to higher irradiation doses, between 150 and 200 ppm. While working at 2000 ppm oxygen a level of conductance equivalent to that of hydrated Nafion<sup>®</sup>117 is maintained at an exposure dose of 200  $\mu\text{C cm}^{-2}$ .

From these data we can conclude that it is possible to maintain the conductivity of the film at higher exposure doses by increasing the oxygen levels during exposure, proving that replacement of the hydrophilic Nafion<sup>®</sup> side chains with their terminal  $\text{SO}_3^-$  moieties by the smaller  $-\text{CO}_2\text{H}$  group in the surface pores of the ion channels is possible without penalty in terms of conductivity.

Returning to consider IR reflectance (ATR) data, we can see that the results of  $-\text{CO}_2\text{H}$  group formation mirror the conductivity properties of the materials described above. We observe a significant difference between the films exposed at 50 ppm oxygen against those treated at higher levels. Fig. 11 shows comparative peak intensities for signals at  $1770\text{ cm}^{-1}$ , assigned to the  $\text{C}=\text{O}$  grouping of the carboxylic acid moiety, for experiments carried out at 50, 550 and 2000 ppm oxygen levels, at exposure doses up to 200  $\mu\text{C cm}^{-2}$ . This data was recorded directly after EB exposure, with no post-irradiation treatment.

Fig. 11 shows that as we increase the availability of oxygen we see a distinct increase in the level of carboxylic acid formation at the site of the polymer backbone, and this is most pronounced when initially raising the concentration from 50 to 550 ppm. This observation supports the theory that the presence of oxygen was the limiting factor for our previous experimental conditions, the mechanism for which is described in Fig. 8.

It has been shown that loss of the hydrophilic side chain of Nafion<sup>®</sup>, as a direct result of EB exposure, is also a major contributing factor to the conductivity of the polymer membrane. The degree of cleavage can be quantified by comparing the intensity of signals for the peaks assigned to the  $\text{C}-\text{O}-\text{C}$  units of the side chain under different experimental conditions. Adjusting the peak intensity for 0  $\mu\text{C cm}^{-2}$  dose

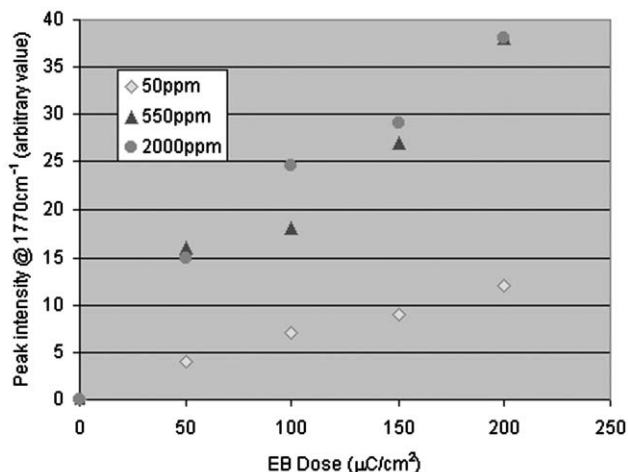


Fig. 11 Comparative peak intensity at  $1770\text{ cm}^{-1}$  for samples at 50, 550 and 2000 ppm oxygen.

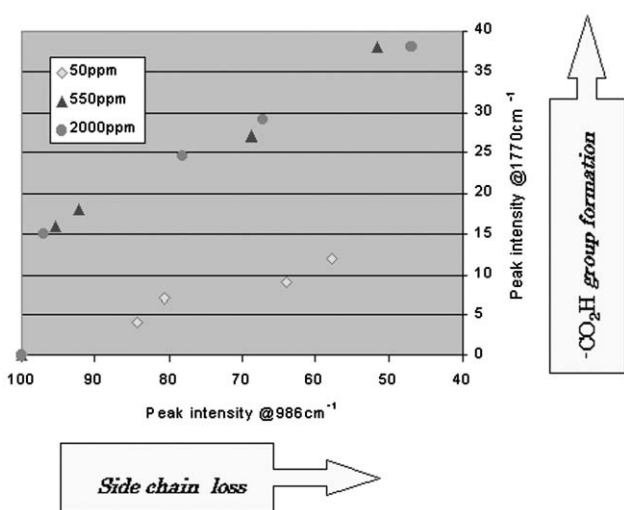


Fig. 12 Formation of  $-\text{CO}_2\text{H}$  ( $1770\text{ cm}^{-1}$ ) units in the Nafion<sup>®</sup> polymer backbone versus loss of side chain ( $986\text{ cm}^{-1}$ ).

to 100% allows us to make a direct comparison between these spectra.

Fig. 12 shows the relationship between the loss of the hydrophilic  $(-\text{OCF}_2\text{-C}(\text{CF}_3)\text{-F})_n\text{-OCF}_2\text{CF}_2\text{-SO}_3\text{H}$  side chain of Nafion<sup>®</sup> and the introduction of carboxylic acid units at the site of the polymer backbone.

Clearly at 2000 ppm the system is saturated with oxygen and we observe a linear relationship between side chain cleavage and carboxylic acid generation. This corresponds with initial expectations, as the point of cleavage of the side chain from the PTFE backbone being the proposed site of subsequent  $-\text{CO}_2\text{H}$  unit introduction.

The effect of oxygen concentration can also be considered in terms of the hydration properties of the film; including post-irradiation water content and uptake capacity. From previous data analysis we can conclude that both the reaction mechanisms for EB irradiation proposed here have an active influence on water management within the film.<sup>18</sup> Here we present conclusions drawn from the analysis of a series of IR spectra, taken at the three different experimental stages (discussed earlier section 2.2), under 50 ppm, 550 ppm and 2000 ppm oxygen. Regarding the IR vibrational modes of water observed for films in their hydrated state, the peaks of interest include the broad band centred at  $3400\text{ cm}^{-1}$ , assigned to the O–H stretching modes, while the O–H bending vibration is visible centred at  $1640\text{ cm}^{-1}$ . However by comparison of the signal intensities of peaks, assigned to the vibrational

modes of  $\text{H}_2\text{O}$ , with those indicative of loss of Nafion<sup>®</sup> side chain and formation of  $-\text{CO}_2\text{H}$  units at the site of the polymer backbone we failed to establish any conclusive relationship. This was also the case for water content data calculated from comparative film dimensions and weight in the hydrated state and after subsequent heat treatment with respect to EB exposure conditions. Simply we can however conclude that generally at high oxygen concentrations (2000 ppm), both water content and uptake capacity are greater than for films irradiated at 50 ppm. This observation is supported by the increase in film conductivity reported for samples irradiated in the presence of increasing oxygen levels;  $50\text{ ppm} \ll 550\text{ ppm} \ll 2000\text{ ppm}$ , Fig. 10.

#### 4. Conclusions

In summary we can conclude that low dose EB exposure facilitates replacement of the sulfuric acid moieties, located at the terminus of the Nafion<sup>®</sup> side chain, with carboxylic acid units as the dominant hydrophilic group found in the pores of the ion channels at the Nafion<sup>®</sup> surface. It has been demonstrated that by increasing the degree of carboxylic acid formation at the site of the polymer backbone the conductivity of the resultant material can be buffered sufficiently so as to compensate for the effect of the subsequent cleavage of the hydrophilic side chains. This result not only confirms the irradiation mechanism postulated but allows significant advantage in the development of membranes with properties optimised for DMFC performance.

#### Acknowledgement

This work was carried out at Toshiba Corporate Research and Development Centre by LJH under the Toshiba Fellowship Program.

#### References

- 1 B. D. McNicol, D. A. J. Rand and K. R. Williams, *J. Power Sources*, 1999, **83**, 15.
- 2 A. K. Shula, M. K. Ravikumar and K. S. Gandhi, *J. Solid State Electrochem.*, 1998, **2**, 117.
- 3 M. Ciureanu, *Proceedings of the 4th International Symposium on New Materials for Electrochemical Systems*, Montreal 9–13th July 2001, Page 268.
- 4 H. Ohzu, *Proceedings of the 2nd Annual Advances in R&D for the Commercialisation of Small Fuel Cells and Battery Technologies for use in Portable Applications*, New Orleans, LA, April 26–28, 2000.
- 5 H. Chang and S. Y. Yoon, *Proceedings of the 4th International Symposium on New Materials for Electrochemical Systems*, Montreal 9–13th July 2001, Page 7.
- 6 A. Heinzl and V. M. Barragan, *J. Power Sources*, 1999, **84**, 70.
- 7 X. Ren, P. Zelenay, S. Thomas, J. Davey and S. Gottesfeld, *J. Power Sources*, 2000, **86**, 11.
- 8 C. Heitner-Wirguin, *Polymer*, 1979, **20**, 371.
- 9 M. A. F. Robertson and K. A. Mauritz, *J. Polym. Sci., Part B: Polym. Phys. Ed.*, 1998, **36**, 595.
- 10 R. M. Blanchard and R. G. Nuzzo, *J. Polym. Sci., Part B: Polym. Phys. Ed.*, 2000, **38**, 1512.
- 11 H. S. Sodaye, P. K. Pujari, A. Goswami and S. B. Manohar, *J. Polym. Sci., Part B: Polym. Phys. Ed.*, 1997, **35**, 771.
- 12 A. Lehmani, S. Durand-Vidal and P. Turq, *J. Appl. Polym. Sci.*, 1998, **68**, 503.
- 13 T. D. Gierke, G. E. Munn and F. C. Wilson, *J. Polym. Sci., Polym. Phys. Ed.*, 1981, **19**, 1687.
- 14 M. Fujimura, T. Hashimoto and H. Kawai, *Macromolecules*, 1981, **14**, 1309; 1982, **15**, 136.
- 15 J. H. G. van der Stegen, J. Görtzen and J. A. M. Kuipers, *J. Membrane Sci.*, 2001, **183**, 61.
- 16 L. J. Hobson, H. Oozu, M. Yamaguchi and H. Hayase, *Proceedings of the 4th International Symposium on New Materials for Electrochemical Systems*, Montreal 9–13th July 2001, Page 379.

- 17 L. J. Hobson, H. Oozu, M. Yamaguchi and H. Hayase, *J. Electrochem. Soc.*, 2001, **148**(10), 1185.
- 18 L. J. Hobson, H. Oozu, M. Yamaguchi and H. Hayase, *J. New Mater. Electrochem. Syst.*, 2001, submitted.
- 19 L. J. Hobson, H. Ozu, Y. Nakano and S. Hayase, *J. Power Sources*, 2002, in press.
- 20 M. Walker, K. M. Baumgartner, M. Kaiser, J. Kerres, A. Ullrich and E. Rauchle, *J. Appl. Polym. Sci.*, 1999, **74**, 67.
- 21 G. Deluga and B. S. Pivovar, *Proceedings of The 3rd International Symposium on New Materials for Electrochemical Systems*, Montreal, QC, Canada, July 4-8, 1999, Ed. O. Savadogo, p.132-135, 1999.
- 22 X. Ren, M. S. Wilson and S. Gottesfeld, *J. Electrochem. Soc.*, 1996, **143**, 1, L12.
- 23 S. Banerjee, *Proc. Power Sources Conf.*, 1994, **36**, 93.
- 24 W. K. Fisher and J. C. Cornelli, *J. Polym. Sci., Polym. Chem. Ed.*, 1981, **19**, 2465.
- 25 K. Schierholz, U. Lappan and K. Lunkwitz, *Nucl. Instrum. Methods Phys. Res., Sect. B*, 1999, **151**, 232.
- 26 U. Lappan, U. Geißler and K. Lunkwitz, *Nucl. Instrum. Methods Phys. Res., Sect. B*, 1999, **151**, 222.
- 27 U. Lappan, U. Geißler and K. Lunkwitz, *J. Appl. Polym. Sci.*, 1999, **74**, 1571.